# PROBABILISTIC SEISMIC VULNERABILITY ANALYSIS OF REINFORCED CONCRETE COLUMNS

VLAD CEANGU , DAN CRETU

*Abstract*. Estimating the response of reinforced concrete columns to a transitory action, represented by a ground motion, is an uncertain task. The randomness of the seismic event and that of the response should be accounted for. The probabilistic seismic vulnerability analysis is a method that one can use for estimating confidence intervals for the response of reinforced columns. In this paper a mixed method using numerical analysis results coupled with experimental data is used for the assessment of the vulnerability of reinforced concrete columns.

*Key words:* performance based earthquake engineering, vulnerability of reinforced concrete columns, seismic demand analysis, ductility of reinforced concrete columns.

## 1. INTRODUCTION

In earthquake engineering the assessment of the response of reinforced concrete columns suppose that at different limit states, which have a particular damage measure *DM*, a mean annual frequency of exceedance is associated. These limit states are chosen as different observable events for the behavior of reinforced concrete columns at a cyclic action [5]. Each limit state has a particular description and an associated intervention cost. The mean annual frequency of the necessary intervention cost is an output of the performance based earthquake engineering procedure.

The limit states used for approximating the vulnerability of reinforced concrete columns are of two categories, according to including or not the collapse of the specimen. The description of these limit states is found in experimental reports or data-bases of such reports. In this paper the data-base used is that presented in [1], using the data for the rectangular columns, with some replacements and adjustments from [3]. The total number of columns used is 272 with the following described limit states: (1) crushing of concrete cover, (2) spalling of concrete cover, (3) buckling of longitudinal reinforcement, (4) rupture of longitudinal reinforcement, (5) rupture of transversal reinforcement, (6) loss of axial strength and (7) element failure. The first three limit states are non-collapse

Technical University of Civil Engineering Bucharest, Romania

Ro. J. Techn. Sci. – Appl. Mechanics, Vol. 63, N° 2, P. 105–121, Bucharest, 2018

states, the rest have associated the element failure (7) state. It is noted that not all columns presented in the data-base have these limit states noted or observed, and in some cases geometrical or material data is missing.

For each column used from the data-base a force-displacement experiment data-file is provided. The cyclic displacement is that of a cantilever column with an axial load applied at the top. The data is transformed for columns with other configurations. Second-order effects are not included to the force-displacement data. The cyclic action is applied at a particular point on the height of the column, and the measured or the effective length of the column is determined from that point to the fixed base. The associated ductility, the hysteretic dissipated energy and other parameters are approximated using the available experimental data.

Using the parameters from the data-base and a numerical model, a fragility curve is approximated for each limit state. The fragility curve developed in this paper represent the variability observed from the experiments for one particular limit state and that of the numerical model used to approximate the particular limit state. The mean annual frequency of exceedance of one particular limit state is as follows:

$$\lambda_{DM} = \int P[DM > y \mid EDP = z] \, \mathrm{d}\lambda_{EDP}(z) \tag{1}$$

where $P[DM > y \mid EDP = z]$ is the fragility curve expressed as the probability of a damage measure *DM* exceeding a particular value *y* when an engineering demand parameter *EDP* is equal to the value *z* associated to one limit state. The second term $\mathrm{d}\lambda_{EDP}(z)$ is the differential variation of the mean annual frequency of exceedance in point *z* approximated by using the probabilistic seismic demand analysis *PSDA* [13]. This quantity is estimated based on the values of intensity seismic measures from a probabilistic hazard analysis and is approximated using the following equation:

$$\lambda_{EDP} = \int P[EDP > z \mid IM = im] \, \mathrm{d}\lambda_{IM} \tag{2}$$

where $P[EDP > z \mid IM = im]$ is the probability of an engineering demand parameter to exceed some value given an intensity measure *IM* equal to a particular *im* value. This term is approximated by using methods of structural engineering such as incremental dynamic analysis [15] or those based on selection of appropriate ground motions [13]. The second term $\mathrm{d}\lambda_{IM}$ is the differential variation of the seismic hazard curve approximated for the equivalent linear single degree of freedom system with period *T*.

Equation (1) is generally numerically solved as a function of the seismic intensity measure *IM* and the damage measure hazard curve *DMHC* is approximated by using the following form [7]:

$$\lambda_{DM} = \lambda_{M_{w,\min}} \sum_i \sum_j \sum_k P[DM > dm_i \mid DM = dm_i]\, P[DM = dm_i \mid EDP = edp_j]$$
$$P[EDP = edp_j \mid IM = im_k]\, P[IM = im_k] \quad (3)$$

The first right term of equation (3), $\lambda_{M_{w,\min}}$, is the mean annual frequency of earthquakes with a magnitude chosen equal to the minimum one [10].

To evaluate the vulnerability of reinforced concrete columns, three particular procedures are followed. The first is the probabilistic seismic analysis *PSHA* which approximates *IM* values from a seismic hazard curve *SHC*, the second is the probabilistic seismic demand *PSDA* analysis which approximates *EDP* values from a seismic demand hazard curve *SDHC* using the results from *PSHA* analysis and the third is the probabilistic seismic vulnerability analysis *PSVA* which approximates *DM* values from a damage measure hazard curve *DMHC*. The vulnerability of reinforced concrete columns is expressed as the mean annual frequency of exceeding a given limit state.

## 2. DATA-BASE OF REINFORCED CONCRETE COLUMNS

The concrete columns available in the data-base have different geometry, type and reinforcement ratios, loading conditions and general behavior. The majority of these columns have a flexural type failure with softening behavior after the peak force and all columns have transverse reinforcement. The concrete used for the columns is normal or high strength concrete, with ductile reinforcement. The values of the yield strength and ultimate strength of the used materials are provided by the authors of the experiments, and as mentioned earlier some values are missing. In the following table, general information about the geometry, materials and general type of columns used are presented.

*Table 1*

General information for the rectangular concrete columns

| | Mean | Standard deviation | Covariance |
|---|---|---|---|
| $L$ [mm] | 1086 | 530 | 0.488 |
| $h$ [mm] | 320 | 122 | 0.381 |
| $f_c$ [MPa] | 51 | 28.6 | 0.561 |
| $f_{ybl}$ [MPa] | 434 | 59 | 0.136 |
| $f_{yew}$ [MPa] | 483 | 215 | 0.445 |
| $n$ | 0.258 | 0.196 | 0.760 |

| P-Δ | 1 | 2 | 3 | 4 |
|---|---|---|---|---|
| | 76 | 137 | 50 | 7 |
| Config. | C | DC | DE | |
| | 104 | 85 | 83 | |
| Failure Type | Flexure | Shear | F-S | |
| | 209 | 23 | 40 | |
| $\rho_l$ [%] | Mean | Std. | Cov. | |
| | 2.767 | 1.197 | 0.432 | |
| $\rho_{ew}$ [%] | Mean | Std. | Cov. | |
| | 0.794 | 0.5 | 0.631 | |

The abbreviations of the configuration types have the meaning of C – cantilever, DC – double cantilever, DE – double ended (clamped at both ends). The types of P-Δ configurations are consistent with the way the vertical and lateral load are applied [1], types one and two correspond to the cases when the effective horizontal force is computed from the second order effects, or as the one given by the authors of experiments in the second case.

There are eight types of confinement configurations, usually one rectangular tie around the perimeter with or without supplemental ties arranged in different ways. The number of ties on each face is given in the data-base and so the compressive strength and ultimate strain of confined concrete is approximated using two models, the model from [9] for normal concrete and the model from [6] for high strength concrete.

Using the force – displacement text files given for each experiment the normalized hysteretic energy is approximated as the ratio between the dissipated energy in one complete cycle to that of the corresponding perfect plastic model in one cycle. For each column the area from the reported cyclic loops is computed and based on the maximum and minimum cycle force and displacement the area of the loop of the perfect plastic model is approximated.

To estimate the ductility of the columns an approximate procedure is used based on the usage of backbone curves. These backbone curves are approximated fitting the following equations on the force - displacement data for each column:

$$f / f_{\max} = \theta_1 \left[ 1 - \left(1 - d/d_{\max}\right)^{\theta_2} \right], \quad d \le d_{\max} \tag{4}$$

$$f / f_{\max} = 1 \Big/ \left[ 1 + \theta_3 \left( d/d_{\max} \right)^{\theta_4} \right], \quad d \le d_{ul}$$

where $\theta_i$ are coefficients evaluated by nonlinear regression, $d_{\max}$ is the displacement associated with the maximum observed force and $d_{ul}$ is the displacement recorded in the last cycle, considered as the maximum allowable displacement if it is not reported by the authors of the experiment.

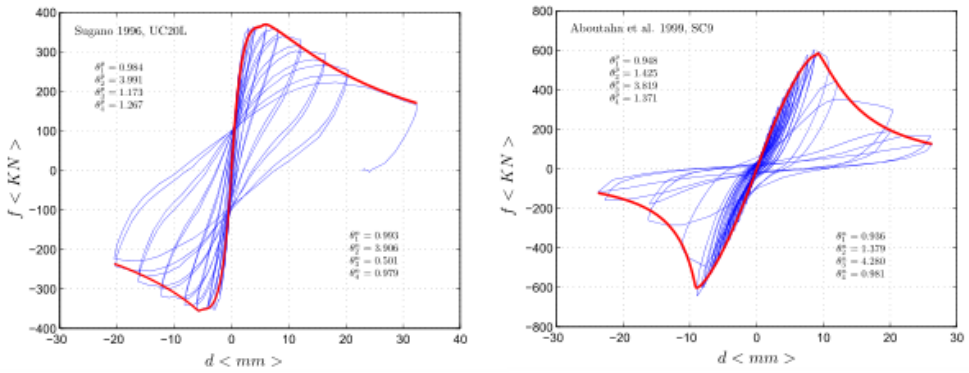


Fig. 1 – Backbone curves of two reinforced concrete columns.

Using equation (4) and the force – displacement data of two columns from the database, the backbone curves from Figure 1 are approximated. These curves are representative as a monotonic incremental load applied at the end of the cantilever versus the measured displacement. The two intervals of equation (4) are a function of $f_{\max}$ and so three modes of plastic behavior can be considered: hardening, approximately elasto-perfect-plastic and softening. In Figure 1 only the softening behavior is plotted.

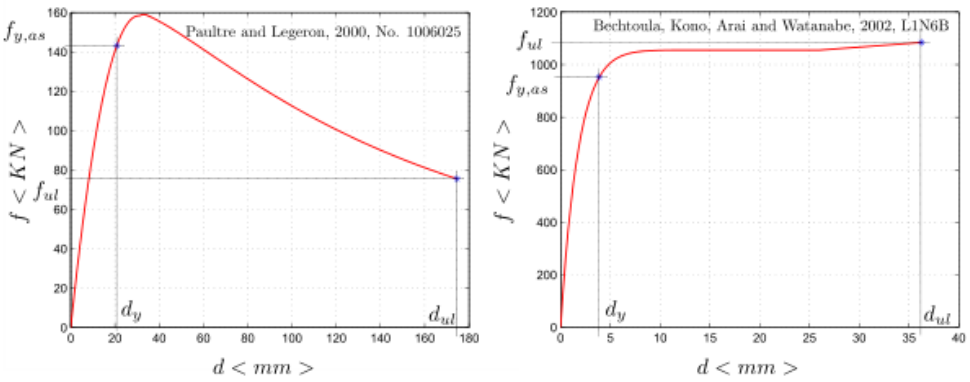


Fig. 2 – Characteristic yield point.

In Figure 2 the used characteristic yield point is represented. Based on the backbone curves of the force-displacement data, an equivalent yield point is chosen as the drop of lateral stiffness of 90%. Effectively the yield displacement corresponding to the point when the ratio of the effective tangent stiffness and the initial tangent stiffness is less than 10%, where the tangent stiffness

$k_{\mathrm{tg},i} = (\partial f / \partial d)_i$ is evaluated using equation (4). Based on this point, an effective yield moment and displacement is approximated.

From the above procedure for each column the dissipated hysteretic normalized energy $E_{h,\mathrm{norm}}$ and the equivalently observed maximum attained ductility $\mu_c$ are approximated. These two parameters are considered response parameters as engineering demand parameters *EDP*, in Table 2 the coefficient of correlation between these parameters and some of the input variables are given:

*Table 2*

Correlation coefficients between the response parameters $\mu_c$, $E_{h,\mathrm{norm}}$ and the column parameters

| | $L/h$ | $f_c$ | $\alpha_s$ | $\rho_l$ | $\rho_{ew}$ | $n$ | $k_{conf}$ | $\mu$ | $E_{h,\mathrm{norm}}$ |
|---|---|---|---|---|---|---|---|---|---|
| $\mu_c$ | 0.122 | 0.172 | −0.043 | −0.081 | 0.265 | 0.039 | 0.372 | 1.000 | 0.305 |
| $E_{h,\mathrm{norm}}$ | 0.197 | 0.135 | −0.373 | 0.277 | 0.298 | 0.098 | 0.248 | 0.305 | 1.000 |

The input variables in percentages used are: $\alpha_s$ for the reinforcement steel, the transversal and longitudinal reinforcement ratios $\rho_{ew}$ and $\rho_l$, the normalized axial force $n$, the confinement efficiency factor $k_{conf}$ defined as the ratio of maximum stress of the confined concrete to the unconfined one, the concrete characteristic strength $f_c$ and the shear span to section height ratio $L/h$. In the following two figures the correlation between some of the input parameters, the response factors and the observed type of failure is plotted [3].

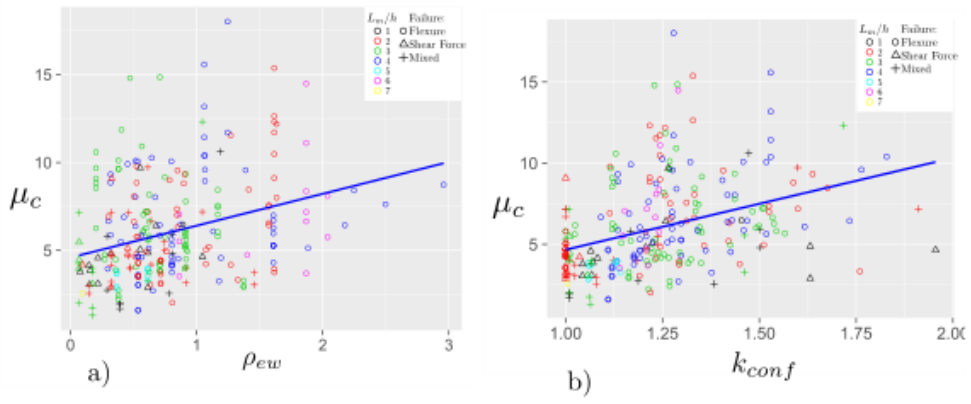


Fig. 3 – Maximum ductility $\mu_c$ as a function of: a) transverse reinforcement ratio $\rho_{ew}$ and b) confinement efficiency coefficient $k_{conf}$.

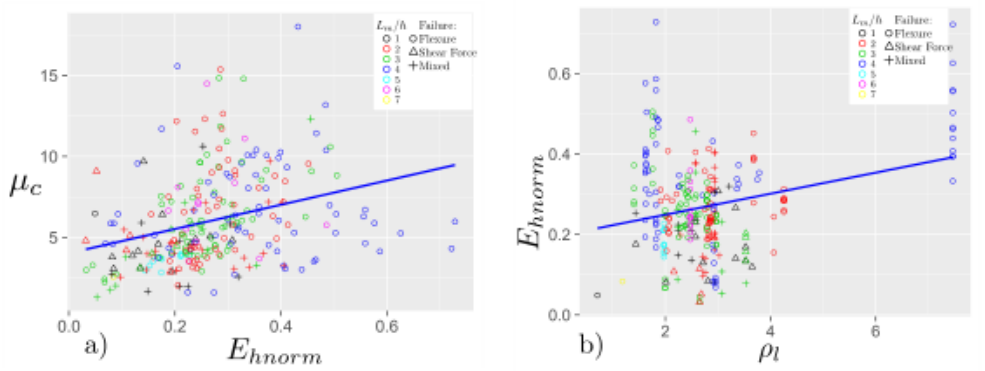


Fig. 4 – a) Maximum ductility $\mu_c$ as a function of normalized hysteretic energy $E_{h,\text{norm}}$ and b) normalized hysteretic energy $E_{h,\text{norm}}$ as a function of the longitudinal reinforcement ratio $\rho_l$.

From Figure 3, it is observed that the estimated ductility of reinforced concrete columns is increasing as the transversal reinforcement ratio $\rho_{ew}$ and the confinement efficiency coefficient $k_{conf}$ increases. For short elements, the values approximated tend to be smaller than the mean values and the majority of these elements have a shear failure type. Generally, elements that exhibit mixed or shear failure type have lower values of transverse reinforcement ratios and confinement efficiency coefficients. Nonetheless, for some elements with mixed or shear failure type high ductility values are observed. Figure 4a shows that the approximated ductility increases as the normalized hysteretic energy is increasing and that the shear and mixed failure modes have the smaller values of the ductility and normalized hysteretic energy. Figure 4b shows that the approximated normalized hysteretic energy is a function of the ratio of longitudinal reinforcement $\rho_l$ also.

With the geometrical characteristics and material properties given or computed based on data given in the data-base, an numerical model is assembled for approximating engineering demand parameters.

The finite element model used for the columns is the force-based beam-column element [12,14] coupled with hinges for the interaction of bending moment with shear force or/and axial force [5,8], strain penetration material models and loss of anchorage or buckling [17]. These elements are implemented in the *OpenSees* framework [11]. The fiber sections mesh dimensions and the number of interpolation points used are those recommended in [2].

The type of analysis employed is the transient analysis with the displacements from experiment applied at the top node of each numerical model of the column. The same displacements, but other forces and hysteretic energy will be obtained. The results from the numerical analysis compared to that approximated from the experimental data are plotted in Figure 5 for two numerical models. The first model considers that the concrete constitutive law without tension strength, the

second model considers it with tension strength and both models do not account for the shear-flexure interaction.

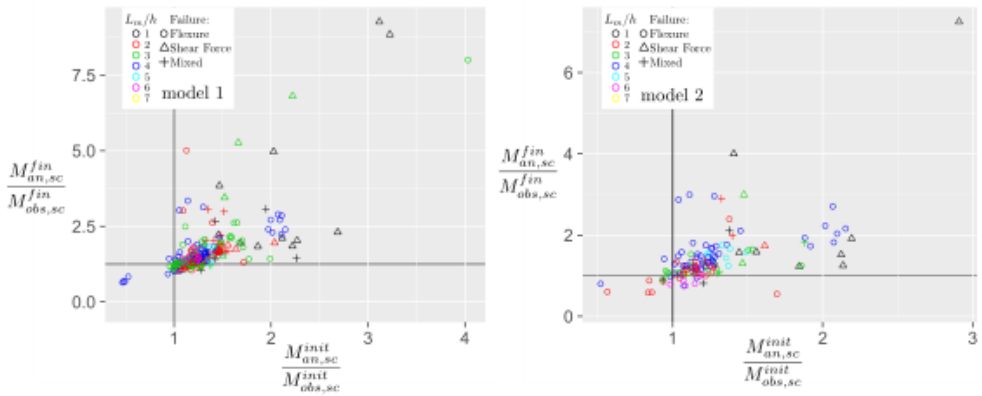


Fig. 5 – Ratio between the numerical approximated bending moment and experimental results for initial and final cycles as function of the maximum force for a) model 1 and b) model 2.

It is observed in Figure 5 that the mean values of the ratios between the numerical approximated and experimental results are 1.26 for flexural failure and 1.40 for mixed failure. For shear failure the mean ratio is 1.90. Using the interaction hinge for shear-bending component, the mean ratio decreases to 1.43. The limit states mentioned in the first section will be numerically evaluated using the displacements corresponding to the strains associated to these limit states [2,4].

The results obtained as ratios from the experimental given data are plotted in Figures 6 and 7. These represent limit states are showed only for specimens that had these limit states reported.

These reported limit states have different influence in the behavior of columns at cyclic action. One column has multiple consecutive limit states before collapsing, or it exhibits at collapse only one type of limit state or a combined state. This is a function of the failure model. If a specimen has a flexure type failure, then it can exhibit multiple limit states. If the specimen has a shear type failure then, generally, it exhibits only one or few limit states.

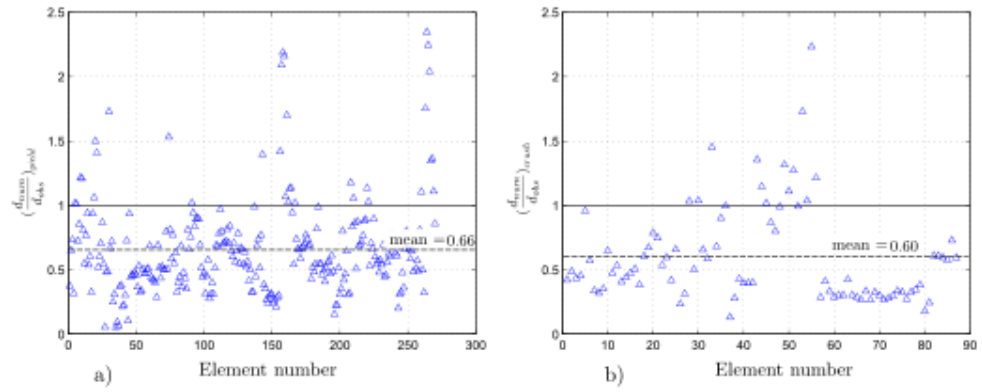


Fig. 6 – Ratios for: a) approximate yield (272 points) and b) crush of concrete cover (105 points).

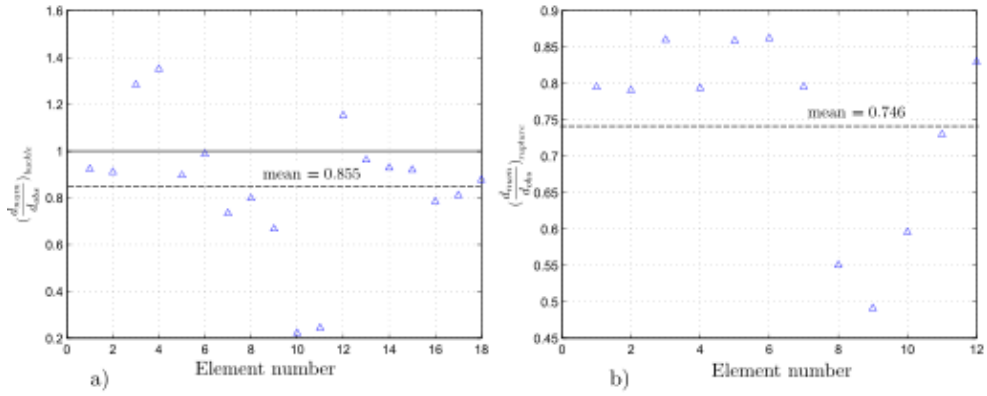


Fig. 7 – Ratios for: a) buckling of longitudinal reinforcement (16 points) and b) rupture of longitudinal reinforcement (11 points).

## 3. FRAGILITY CURVES

Using a mixed method based on the results in the previous section, fragility curves are approximated for five reported limit states of the reinforced concrete columns. Fragility curves are cumulative distribution functions $F_{DM}(dm)$ of a particular damage measure.

To fully define fragility curves, a mean and a standard deviation is approximated. The empiric cumulative distributions of the ratios of numerical estimated ductility to the approximated experimental one is conditioned on the number of available data. The fragility functions used herein describe the aleatory observations of different limit states and the differences observed for the numerical model used.

For each *DM* the empiric cumulative distribution is approximated using the available data and if the data is missing then is considered null because the numeric model doesn't reach that limit state and the collapse is obtained at a different state. Three types of distribution are tested, namely the normal, log-normal and Weibull distributions. The quantitative test for estimation criteria is Kolmogorov-Smirnov with the critical coefficient as a function of the number of data pairs. In Figure 8a the results obtained are presented with their particular critical values.

The values chosen for the critical coefficient $D_{2,cr}$ are for a confidence factor of 95%. As it is observed, the log-normal distribution has the lowest $D_2$ coefficients. The coefficient of variation using the log-normal distribution for each limit state are: $Var_{crush} = 40.9\%$, $Var_{buc} = 12.6\%$, $Var_{rup} = 21.2\%$ and $Var_{r,ew} = 50.8\%$. The ultimate limit state of ties and that of crushing of concrete cover are the most uncertain states.

These curves represent the first term of equation (1) written as follows:

$$P[DM > dm \mid EDP = z] = 1 - \Phi\left(\frac{\ln dm - mean_{\ln DM}}{sd_{\ln DM}}\right) \tag{5}$$

with the mean and standard deviation approximated from each of the fragility curve from Figure 8 for different values of the damage measure.

Reinforced concrete columns can have collapse which is achieved at a particular limit state. The probability of appearance of a limit state $P(LS)$ is equal to the number of observations of that limit state from the total number of observations.

The complete fragility model is obtained considering the probability that the expected ductility is equal to that associated with the ductility of the limit state and the expected one expressed as the multivariate distribution $P[DM=dm, EDP=edp]$. This distribution is obtained as the product of the distribution of *DM*, $P[DM = dm \mid EDP_{SL} = edp]$, and the distribution of *EDP* at a particular limit state $P[EDP=edp]$. The sum of this joint distribution is almost equal to one and it can be obtained for each limit state. In Figure 9 an example of two distributions is given. It is observed that the variability considered for the limit state is less than that of $EDP_{SL} = edp$.

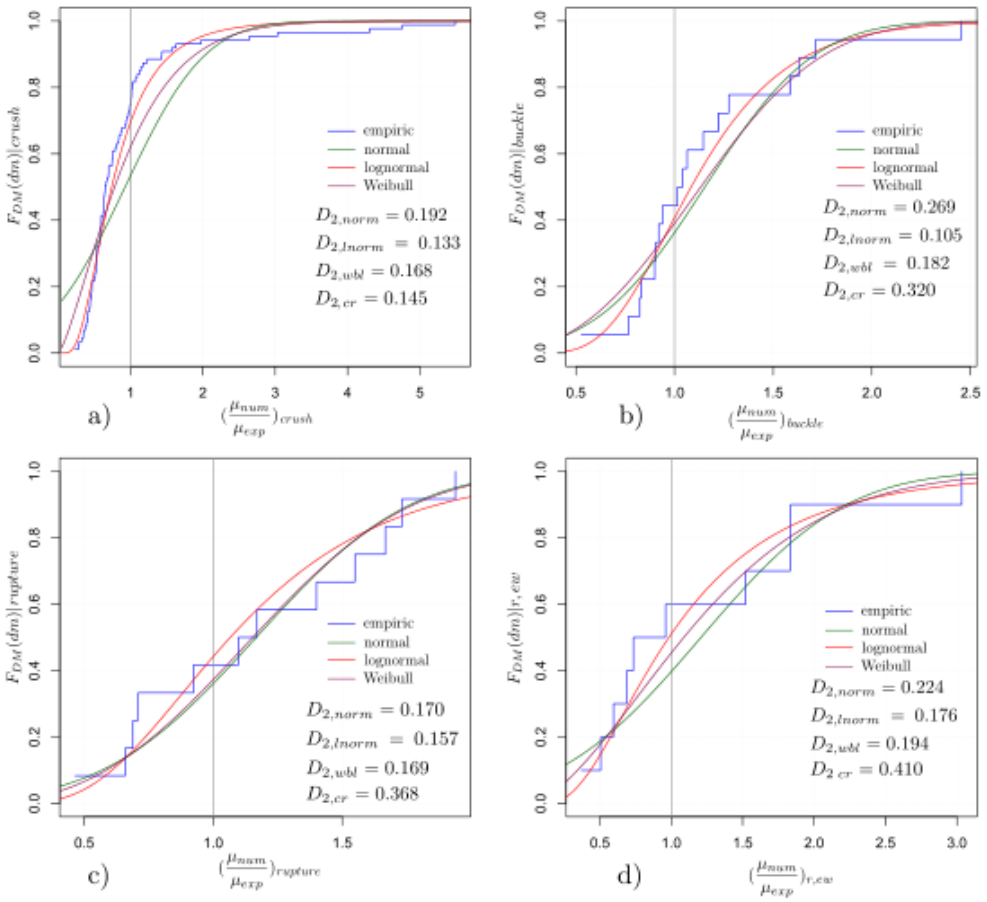


Fig. 8 – Fragility curves for: a) crushing of concrete cover, b) buckling of longitudinal reinforcement, c) rupture of longitudinal reinforcement and d) rupture of ties.

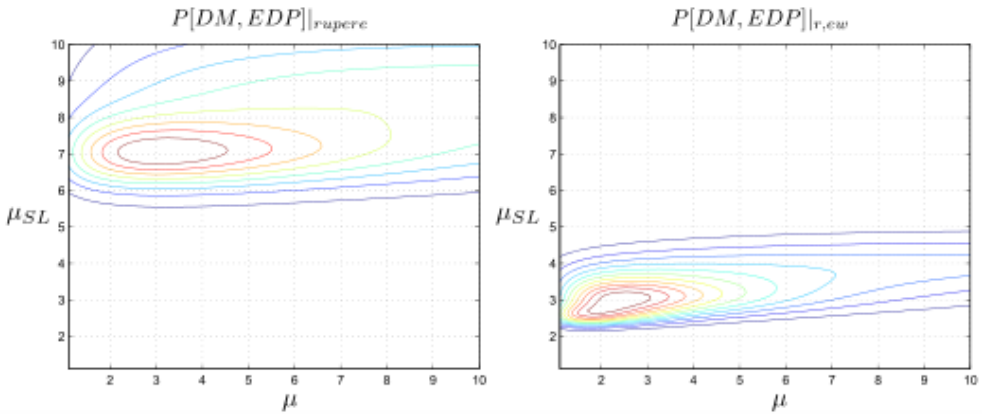


Fig. 9 – Joint log-normal distribution of $P[DM, EDP]$.

The observed limit states in the joint distribution $P[DM = dm \mid EDP_{SL} = edp]$ are included in the form:

$$P[DM = dm \mid EDP_{SL}] = (1 - P[SL])\, P[DM = dm \mid EDP_{SL}, nSL] + \\ + P[SL]\, P[DM = dm \mid EDP_{SL}, SL] \quad (6)$$

where $P[DM = dm \mid EDP_{SL}, nSL]$ if the probability that *DM* is equal to a particular value when *EDP* is not equal to $EDP_{SL}$ – the value associated to a particular limit state.

## 4. PROBABILISTIC SEISMIC VULNERABILITY ANALYSIS

To approximate the mean annual frequency of exceedance of an particular *DM* value it is necessary to evaluate the mean rate of occurrence of *EDP* values. This procedure is called probabilistic seismic demand analysis (*PSDA*) and is solved by using equation (2) and the numerical model presented in the section above. Engineering demand parameters are estimated using values from a seismic demand hazard curve *SDHC*.

### 4.1. Seismic action

The method for selecting ground motions used herein is based on the condition that the elastic and inelastic spectra of the selected records to be similar to that of the spectra of the accelerogram recorded at the INCERC station in 04.03.1977 after the Vrancea event. These records are selected from the *ROMPLUS* and *PEER* data-base and in total a number of 15 accelerograms are chosen. These used ground motions have the property that the frequency content is similar to that of the selected reference one. These accelerograms are scaled linearly to different hazard levels corresponding to a seismic hazard curve.

The seismic hazard curve is obtained using a probabilistic seismic hazard analysis with the Cornell-Mcguire method [10] for a fictitious site, situated at 100 km from the Vrancea source on a soft soil site, with intensity measures approximated using the ground motion model proposed by [16]. The derivate of the hazard curve is obtained using the format proposed by Kennedy and Short [7]. In figure 10, the elastic spectra of the accelerograms and a typical hazard curve and its derivate is plotted.

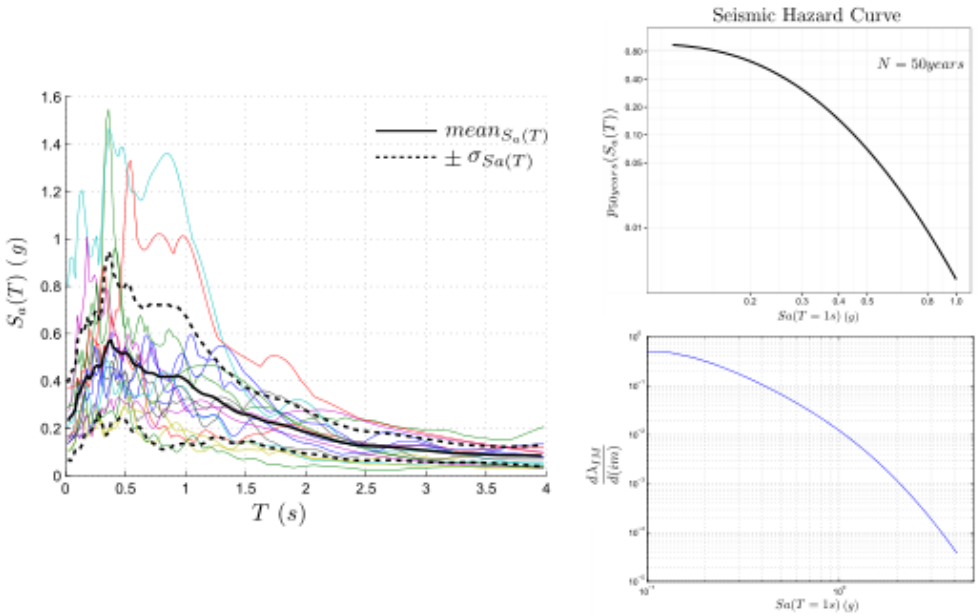


Fig. 10 – Elastic spectra of used accelerograms and the seismic hazard curve and its derivate.

### 4.2. Probabilistic Seismic Demand Analysis

With the information in the previous subsection and using equation (2), the mean annual frequency of exceedance of an engineering demand parameter is estimated. The only unknown quantity is the first term of equation (2), which is approximated using the incremental dynamic analysis [15]. Using the nonlinear mathematical model of the reinforced concrete columns for each accelerogram at each scale factor, a nonlinear dynamic analysis is completed and individual response parameters are obtained. After interpolating the results, a functional is used to approximate the response as a function of *IM* and the *IDA* curve is obtained.

Each point on the *IDA* curve represents the mean value of $\ln IM$ and at this point a particular standard deviation $\sigma_{\ln IM}$ is approximated. A log-normal distribution of a given mean and standard deviation can be given to the values of *EDP* as a function of *IM*, $P[EDP > z \mid IM = im]$. In Figure 11 the *IDA* curve and the seismic demand hazard curve are represented.

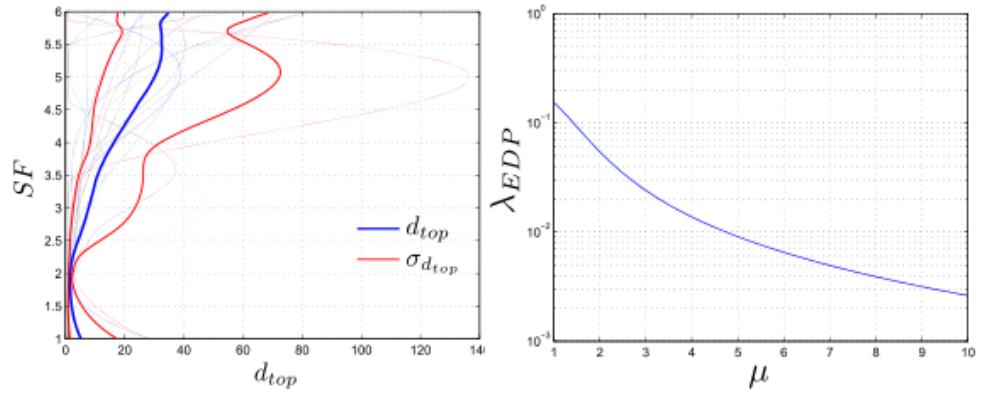


Fig. 11 – *IDA* curve and the seismic demand hazard curve *SDHC*.

The seismic demand hazard curve represents the mean annual frequency of exceedance of a particular *EDP* value for a system exposed to the seismic hazard associated to Vrancea source. These factors have no collapse included and the behavior is not corrected to that of a real system. This kind of analysis gives informations about the numerical response of the chosen type of modeling. In the probabilistic seismic vulnerability analysis the first derivative of $\lambda_{EDP}$ will be approximated by central finite differences.

### 4.3. Assessing vulnerability

Using the results from the *PSDA* analysis, the fragility curves approximated earlier and the total probability theory from equation (1), the mean annual frequency of exceedance of a particular limit state is evaluated. Equation (3) is written in a simplified form as:

$$\lambda_{DM} = \sum_{i=1}^{i=m} P[DM > dm \,|\, EDP = z_i] \cdot \frac{\mathrm{d}\lambda_{EDP}}{\mathrm{d}z}\Big|_{z_i} \tag{7}$$

A number of four columns are chosen from the data-base, with equivalent elastic periods of 0.30s, 0.50s, 0.80s and 1.00s. All these columns exhibit flexural failure and those with periods of 0.30s and 0.50s are stiffer than the other two and have a higher lateral strength. In Figure 12 the *DMHC* curves are plotted.

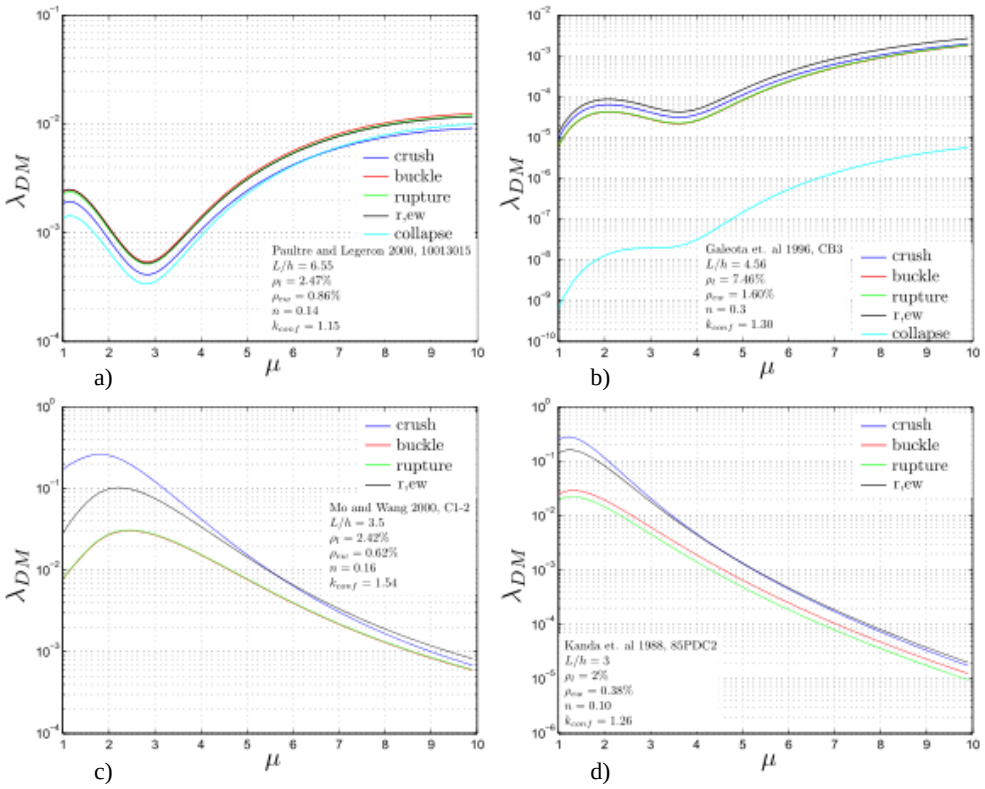


Fig. 12 – *DMHC* curves for four chosen columns from the data-base with equivalent elastic periods: a) 0.8 s; b) 1.0 s; c) 0.3 s; d) 0.5 s.

It is observed that these distributions are a function of the *EDP* values, at each limit state $\lambda_{DM}$ is a function of the appearance of a particular *EDP* value. This value has a recurrence interval for the *DM* values. In the case of weak systems there is no distinction between limit states; the collapse is the reported limit states almost in all cases. For either level of the scaling factors the model will give approximate values in almost all limit states. In the case of rigid systems the observed limit states are different for each scaling interval, so such model could represent the consecutive development of limit states.

The vulnerability assessment is defined as the mean frequency of exceedance $\lambda_{DM}$. The values associated to a particular level of hazard are approximated using the values evaluated in the numerical analysis for each limit state. The values on these curves are defined as local points associated to a limit state.

## 5. CONCLUSIONS

The required steps of the probabilistic seismic vulnerability analysis are given in this paper. The procedure is based on results evaluated using the probabilistic seismic hazard analysis and the probabilistic seismic demand analysis. These two procedures are independent of the vulnerability analysis but are interdependent. The *PSDA* analysis requires data from the *PSHA* analysis.

In the vulnerability assessment the probability of exceedance of a particular value of damage measure is evaluated. This probability is associated to an intensity measure or an engineering demand parameter. Using the damage measure hazard curve the expected damage in a period of time can be estimated or the mean interval of recurrence, $1/\lambda_{DM}$ , for a particular limit state can be approximated. Generally, a greater intensity measure means greater expected damage.

This procedure associates for the engineering demand parameter a quantity to evaluate with confidence the real response of the analyzed element, only if the considered element is similar to the ones in the data-base and that the numerical model is the same with that used to develop the fragility curves. The fragility curves developed herein have the advantage of being calibrated to experimental results so that the localization of the response due to numerical modeling is reduced. These curves can be used for models with the same numerical approximation if the obtained generalization is kept.

By using this kind of procedure, the intervention cost over a period of time can be estimated based on the expected damage measure. The damage measures presented are in general limit states that are observed for the materials of the reinforced concrete column, expressed as damage of concrete or reinforcement. The ductility or dissipated energy are not used as damage measures. The used damage measures can have associated intervention costs.

It was observed that each column will exhibit different limit states, according to its geometry, applied loads and material properties. A general model for drift isn't conservative to be applied. All these columns have different responses, so for assessing their vulnerability, each column should be analyzed. Extrapolating the results can be nonconservative and, in the case of columns that exhibit shear failure, physical unreliable.

*Received on November 2, 2017*

## REFERENCES


1. BERRY, M.P., PARRISH, M., EBERHARD, M.O., *PEER Structural Performance Database, Version 1.0*, 2004.
2. BERRY, M.P., EBERHARD, M.O., *Performance modeling strategies for modern reinforced concrete bridge columns*, Technical Report 2007/07, PEER, April 2008.
3. CEANGU, V., *The influence of mathematical modeling of nonlinear behavior on the seismic response of civil constructions* (in Romanian), PhD Thesis, UTCB, November 2017.
4. CEB/FIP. *Model Code 2010*, 2010.
5. ELWOOD, K.J., MOEHLE, J.P., *Shake table tests and analytical studies on the gravity load collapse of reinforced concrete frames*, Technical Report 2003/01, PEER, November 2003.
6. GALEOTA, D., GIAMMATTEO, M., MARINO, R., *Strength and ductility of confined high strength concrete*, Proceedings of the Tenth World Conference on Earthquake Engineering, Madrid, Spain, vol. 5, pp. 2609–2613, 1992.
7. JALAYER, F., CORNELL, C.A., *A technical framework for probability-based demand and capacity factor design (DCFD) seismic formats*, Technical Report PEER Report 2003/08, University of Berkeley, November 2003.
8. KOLOZVARI, K., ORAKCAL, K., WALLACE, J., *Shear-flexure interaction modeling for reinforced concrete structural walls and columns under reversed cyclic loading*, Technical Report 2015/12, PEER, December 2015.
9. MANDER, J.B., PRIESTLEY, M.J.N., PARK, R., *Theoretical stress-strain model for confined concrete*, Journal of Structural Engineering, **114**, *8*, pp. 1804–1826, 1988.
10. MCGUIRE, R.K., *Seismic hazard and risk analysis*, EERI, MNO-10, 2004.
11. MCKENNA, F., FENVES. G.L., SCOTT, M.H., MAZZONI, S., *Open system for earthquake engineering simulation*, Technical report, PEER, June 2006.
12. SCOTT, M.H., HAMUTÇUOĞLU, O.M., *Numerically consistent regularization of force-based frame elements*, International Journal for Numerical Methods in Engineering, **76**, *1*, pp. 1612–1631, 2008.
13. SHOME, N., CORNELL, C.A., *Probabilistic seismic demand analysis of nonlinear structures*, Technical Report RMS-35, Stanford University, March 1999.
14. SPACONE, E., FILIPPOU, F.C., TAUCER, F., *Fibre beam-column model for non-linear analysis of R/C frames: Part I. Formulation*, Earthquake Engineering and Structural Dynamics, **25**, *1*, pp. 711–725, 1996.
15. VAMVATSIKOS, D., CORNELL, C.A., *Incremental dynamic analysis*, Earthquake Engineering and Structural Dynamics, **31**, *3*, pp. 491–514, 2002.
16. VĂCĂREANU, R., RADULIAN, M., IANCOVICI, M., PAVEL, F., NEAGU, C., *Fore-Arc and Back-Arc ground motion prediction model for Vrancea intermediate-depth seismic source*, Second European Conference in Earthquake Engineering and Seismology (2ECEES), Istanbul, Turkey, August 24-29, 2014..
17. ZHAO, J., SRITHARAN, S., *Modeling of strain penetration effects in fiber-based analysis of reinforced concrete structures*, ACI Structural Journal, **104**, *2*, pp. 133–141, 2007.